WEALDABILITY

Weldability of nickel-base superalloys for energy applications

KME-706

LARS NYBORG AND JOEL ANDERSSON

ISBN 978-91-7673-087-4 | © 2018 ENERGIFORSK

Energiforsk AB | Phone: 08-677 25 30 | E-mail: kontakt@energiforsk.se | www.energiforsk.se

Preface

The project has been performed within the framework of the materials technology research programme KME, Consortium materials technology for thermal energy processes, period 2014-2018. The consortium is at the forefront of developing material technology to create maximum efficiency for energy conversion of renewable fuels and waste. KME has its sights firmly set on continuing to raise the efficiency of long-term sustainable energy as well as ensuring international industrial competitiveness.

KME was established 1997 and is a multi-cliental group of companies over the entire value chain, including stakeholders from the material producers, manufacturers of systems and components for energy conversion and energy industry (utilities), that are interested in materials technology research. In the current programme stage, eight industrial companies and 14 energy companies participate in the consortium. The consortium is managed by Energiforsk.

The programme shall contribute to increasing knowledge within materials technology and process technology development to forward the development of thermal energy processes for efficient utilisation of renewable fuels and waste in power and heat production. The KME goals are to bring about cost-effective materials solutions for improved fuel flexibility, improved operating flexibility, increased availability and power production with low environmental impact.

KME's activities are characterised by long term industry and demand driven research and constitutes an important part of the effort to promote the development of new energy technology with the aim to create value and an economic, environmentally friendly and long term sustainable energy society.

The industry has participated in the project through own investment (60 %) and the Swedish Energy Agency has financed the academic partners (40 %).

Bertil Wahlund, Energiforsk

Abstract

The aim of the project has been to establish knowledge about weldability assessment of Ni-based superalloys. This aim has been broken down into several objectives: Using knowledge obtained from previous KME 506/518 to assess weldability of Ni-based superalloys; Establish knowledge about factors that influence the susceptibility towards strain age cracking (SAC); Investigate general susceptibility of new alloys towards SAC; developing a testing rationale that can provide deeper understanding of ongoing mechanisms; assess how influencing factors can be controlled and how SAC can be prevented.

The results show that weld cracking behaviour is highly alloy specific and no generalized approach is possible to prevent cracking during welding of superalloys. More specifically, ATI 718Plus is more susceptible towards HAZ liquation cracking than Haynes 282, while for the latter the concern was mainly solidification cracking.

The strain age cracking susceptibility of different alloys has been investigated, with Haynes 282 showing comparable resistance to Alloy 718. Furthermore, the precipitation characteristics of Haynes 282 could be correlated to the low ductility responsible for strain age cracking to occur via a newly developed testing procedure.

Sammanfattning

Ökande användningstemperaturer och intermittent användning av landbaserade gas och ångturbiner är starka drivkrafter till forskning på nickelbaserade superlegeringar. Syftet med projektet var att grundläggande studera och öka kunskapen om svetssprickor med fokus på de så kallade töjnings-åldringssprickorna. Syftet har även varit att utveckla ett testförfarande för att kunna förutse uppkomsten av spricktypen och dess underliggande mekanismer.

Projektet, KME 706, har inom ramen för KME utförts i samarbete mellan Chalmers Tekniska Högskola och GKN Aerospace Sweden AB. Referensgruppen bestod av deltagare från båda parter. Genom att undersöka mikrostrukturen från flerlagersvetsning så kunde sprickkänsligheten hos ATI 718Plus och Haynes 282 utvärderas. Utvecklingen av en testmetod för att prediktera känslighet gällande töjnings-åldringssprickor med hjälp av en så kallad Gleeblemaskin tillsammans med omfattande karaktärisering av mikrostruktur har utgjort en stor del av forskningsarbetet.

Det övergripande målet att grundläggande förstå mekanismerna gällande svetssprickor i utskiljningshärdande nickelbaserade superlegeringar har lyckats genom att kombinera omfattande metallurgiska undersökningar i kombination med svetsbarhetsstudier och utveckling av tillförlitliga testförfaranden. Projektet resulterade i 8 st vetenskapligt granskade tidsskrifts- och konferensartiklar. Projektet har dessutom resulterat i olika samarbeten med både nationellt och internationellt erkända aktörer vilket stärkt forskningen.

<u>Nyckelord</u>: svetsning, nickelbaserade superlegeringar, svetssprickor, töjnings-åldringssprickor, kallsprickor

Summary

Increasing operating temperatures as well as intermittent cycling of land-based gas and steam turbines motivates research on highly temperature stable alloys such as nickel-based superalloys. The aim of this project was to obtain fundamental knowledge about the formation of weld cracking, including hot cracks but with particular interest in strain age cracking (SAC). This aim has further been divided into weldability testing and the development of dedicated testing procedures to assess the susceptibility towards SAC and to provide further insight into the ongoing mechanisms.

The project KME 706 has within the framework of KME been carried out as a cooperation between Chalmers University of Technology and GKN Aerospace Sweden AB. The reference group included participants of both parties. By investigating the microstructure resulting from multi-pass welding the weld cracking resistance of the newly developed alloys ATI 718Plus and Haynes 282 has been evaluated. The development of test methods to assess the susceptibility towards strain age cracking via Gleeble testing, as well as extensive microstructural characterization have been an integral part of the project.

The overall goal of obtaining fundamental knowledge about weld cracking mechanisms in precipitation hardening nickel based superalloys has been achieved as planned via the combination of extensive metallurgical investigations within the framework of weldability studies and the development of reliable testing procedures. The project led to 8 articles in peer reviewed journals and scientific conferences. The project furthermore led to collaboration with different national and international partners, strengthening existing networks.

Keywords: welding, nickel-based superalloys, weld cracking, strain age cracking, hot cracking

List of contents

1 Introduction

Welding plays a major role in the fabrication of nickel based superalloys. This is based to the possibility to join different materials with small limitations on the shape and previous manufacturing steps. One example is the trend to introduce welding to the fabrication of hot structural parts of jet engines. These components, made out of nickel based superalloys, have traditionally been produced as large cast parts [1]. By using welding as a joining technique, the combination of high-strength wrought parts and complex shaped cast parts is possible and allows for both weight and price reductions [2]. However, besides the anisotropic mechanical properties of welds, also the susceptibility to weld cracking of nickel based superalloys has to be taken into account.

1.1 BACKGROUND

The cracking processes occurring in nickel based superalloys can be divided into different groups, based on the temperature range they occur. Cold cracking is usually not directly connected to welding and includes e.g. hydrogen embrittlement at ambient temperature. Warm cracking phenomena such as strain age cracking and ductility dip cracking occur at high temperatures in the heat affected zone, but do not require a liquid phase to be present. They are hence also referred to as solid state cracking. Hot cracking occurs at high temperatures and requires the presence of liquid phases, with possible crack formation in both the fusion- and heat-affected zone [3]

1.1.1 Hot cracking

Hot cracking can be further divided into two mechanisms, namely weld solidification cracking and heat-affected zone (HAZ) liquation cracking. Weld solidification cracking occurs in the fusion zone, where cracks are formed during the passage of the liquid-solid two-phase region upon cooling. Several theories have been proposed during the last 60 years, but still not all aspects have been fully understood. In general, two main factors can be identified, namely the presence of restraint and a susceptible microstructure. The former can be due to the formation of thermal stresses during cooling, as a temperature and heating/ cooling rate gradient between fusion zone and base material is present. The restraint is further influenced by the weld bead geometry, workpiece design and thickness, heat input during welding and mechanical fixture (external restraint). Early theories include the shrinkage-brittleness theory [4] and the strain theory of hot tearing [5]. These have been combined to the generalised theory of super-solidus cracking by Borland in the early 1960s [6].

In contrast to weld solidification cracking, which occurs in the fusion zone of the weld, HAZ liquation cracking is localised to the partially melted zone, usually referred to as PMZ. This zone lies in the heat affected zone and is in close proximity to the fusion zone. Its main characteristic is the presence of a liquid fraction, forming when exceeding the effective solidus temperature during heating. The presence of stresses during subsequent cooling then can cause crack formation. The liquid can form by different mechanisms, namely segregation induced liquation caused by alloying elements such as S, P and B, constitutional liquation and eutectic melting. The former has extensively been studied for Alloy 718 [7–17]. Constitutional liquation requires fast heating and the presence of secondary phases in the matrix. Due to the fast heating the partial dissolution of particles occurs before diffusion processes can level out local chemical composition around the dissolving particle. Liquid can form if low melting compositions exist in the alloy (e.g. eutectic phases). The mechanism has been originally proposed by Pepe and Savage [18] and later adapted by Owczarski et al. for HAZ liquation cracking in Alloy 718 [19]. Constitutional liquation has been observed especially for Nb bearing alloys such as Alloy 718 and ALLVAC 718Plus [2, 19] but has also been reported for other precipitation hardening alloys [20–23].

Eutectic melting is only found in cast alloys and related to the strong segregation in interdendritic areas. This has been observed in cast Alloy 718 by various authors [2, 24, 25]. Related to the in general more segregated microstructure of cast alloys they have to be considered more susceptible to HAZ liquation cracking.

1.1.2 Strain age cracking

Strain Age Cracking (SAC), also referred to as reheat cracking post weld heat treatment (PWHT) cracking, occurs in precipitation hardening nickel based alloys, mainly in γ' hardening grades [3]. As reheat cracking in steels it occurs during heating to PWHT after welding. Even though some similarities exist, the metallurgy of precipitation hardened nickel based superalloys leads to a different detailed mechanism and influencing factors.

The general mechanism of stain age cracking has been studied in the early 1960s and 70s by various researchers [26–33]. It is generally accepted that the occurrence of cracks during the PWHT cycle is caused by simultaneous presence of stresses in the heat affected zone and a low ductility in this region. This is explained as follows. During cooling from welding a significant amount of restraint is built up in the heat affected zone due to thermal stresses and external weld restraint. The former are caused by the temperature gradient present from base metal to weld fusion zone. The residual stresses are relieved during heating to the PWHT, which coincides with the precipitation of hardening phases (*cf.* Figure 1) [28].

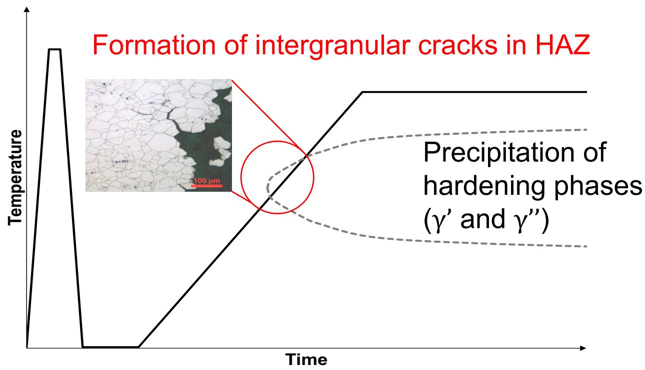

Figure 1: General mechanism of strain age cracking. Fast heating and cooling during the weld thermal cycle, followed by slow heating to post weld heat treatment, where stress relaxation coincides with precipitation of hardening phases and intergranular cracking occurs

The precipitation reaction is believed to lead to a higher strength of the grain interior as compared to the grain boundaries. The deformation (i.e. stress relaxation) is thus localised to the grain boundaries. When grain boundary sliding is not accompanied by volume deformation, high stresses develop especially at grain boundary triple points and intergranular cracks form [34, 35]. Different authors further claim an additional effect of contraction stresses due to γ' precipitation based on the difference in lattice parameter of the γ matrix and γ' [27, 28, 36, 37].

1.2 DESCRIPTION OF THE RESEARCH FIELD

The research focussed on strain age cracking began during the 1960s when cracking problems during post weld heat treatment lead to the development of Alloy 718. Figure 2 shows the total amount of published papers on strain age cracking over the years.

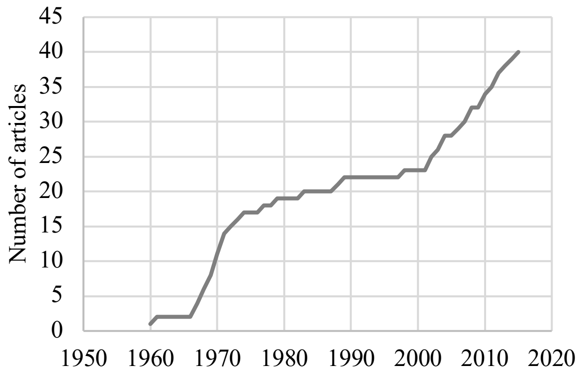

Figure 2: Amount of articles published on strain age cracking (cumulative) [38].

The graphical evaluation shows two time periods with increased research activity. The first one in the late 60s and early 70s covered the development of the general mechanism as well as testing procedures. Over the following years only few publications are available, some of them review articles summarising the current state of research (e.g. Thamburaj et al. 1983 [39]). The second increase in research activity is visible starting from ≈ 2000. Publications in this period mainly cover the development of test methods and rankings of different materials (6 of 17 articles). The alloys being investigated range from the 'standard' grades such as René 41, Waspaloy and Alloy 718 to the more recently developed grades Inconel 738LC (4), Allvac 718Plus (2) and Haynes 282 (3)

1.3 RESEARCH TASKS

The proposed project is a continuation of previous project abbreviated KME 506, in which fundamental aspects on weldability in general and especially hot cracking during welding of Ni-base superalloys were in focus. Within the KME 506 project, the problems associated with strain age cracking (SAC) were slightly touched upon. The SAC is related to precipitation of hardening phases, primarily γ' phase, occurring at heating up to the PWHT temperature, which can cause intergranular cracking in the material. With newly developed alloys such as ATI 718Plus and Haynes 282 and hence limited available data regarding their weldability, the research task is to investigate their weld cracking behaviour with particular interest in their susceptibility towards SAC. Furthermore, while the general mechanism of strain age cracking is not disputed, further research is required to reliably predict the material response after welding and hence the risk towards crack formation.

1.4 GOALS

This research projects' aim is to obtain fundamental knowledge about the formation of weld cracking, including hot cracks but with particular interest in strain age cracking (SAC). The goal has been defined on a more detailed level in form of the following objectives:

1. Clarify the fundamental cause of weld cracking, with focus on strain age cracking

   Goal is largely fulfilled; general welding behaviour was investigated and more knowledge about SAC mechanism has been obtained. Further studies necessary to answer remaining/ new questions

2. Develop a testing rationale to assess susceptibility towards strain age cracking

   Goal fulfilled. A testing procedure for screening purposes has been developed. Furthermore, a test providing insight into SAC mechanism has been proposed and successfully applied. Further R&D work is ongoing.

1.5 PROJECT ORGANISATION

The project is based on cooperation in between Chalmers University of Technology and GKN Aerospace Sweden AB. Professor Olarewaju Ojo at University of Manitoba, Canada, and Prof. Boian Alexandrov at The Ohio State University, USA, have been involved as advisors in the project and have visited several times. The project has been conducted within the framework of KME.

The industrial partner of the project has been GKN Aerospace Sweden AB. The in-kind contribution from GKN is 7 504 470 SEK.

Swedish Energy Agency has financed the project with 5 000 000 SEK assigned to Chalmers University of Technology, constituting a publically funded share of 40%.

The project has been organised by a project management group led by Dr Geraldine Puyoo at GKN Aerospace Sweden AB (Geraldine Puyoo, Bengt Pettersson and Johan Ockborn) were also members from Chalmers University of Technology (Fabian Hanning, PhD student, Joel Andersson and Lars Nyborg, supervisors) have been included. Project management group meetings have been held once per month to review the monthly deliverables as well as other technical aspects. Supervision meetings have been held every second week separately to the project management group meetings.

2 Materials and methods

2.1 ATI 718 PLUS

Investment cast plates with the dimensions 150 x 60 x 62.7 mm and the chemical composition given in Table 1 have been used [40].

Table 1 Chemical composition in weight percentage of cast ATI 718Plus®

Ni	Cr	Co	Mo	Ti	Al	Fe	Mn	Si	C	B	Nb	W
Bal	20.72	8.34	2.71	0.75	1.50	9.31	0.01	0.04	0.05	0.005	6.02	1.00

2.1.1 Repair welding

The plates had an average grain size of 1300 ± 200 µm and a hardness of 415 ± 5 HV0.5. Different homogenisation heat treatments were applied to a subset of the plates, namely 1120, 1160 and 1190°C, with exposure times of 4 and 24h, respectively. These temperatures have been chosen below, at, and above the incipient laves melting temperature of the alloy [41]. While such treatments are commonly applied in conjunction with hot isostatic pressing, the heat treatments were carried out in a small lab furnace at ambient pressure.

Four linear grooves with the dimensions 30 x 10 x 10 mm have subsequently been machined into the plates as shown in Figure 3. The repair welding has been carried out manually by experienced welders, using manual gas tungsten arc welding with a tungsten-2% thorium (WT-20) electrode. The welds were shielded by argon, with a nozzle gas flow of 8–15 l/min. ATI 718Plus® wire with 1.14 mm diameter has been used as filler material. A wide nozzle has been used to create a diffuse gas flow, enabling a large electrode stick-out to reach the bottom of the grooves. Welding current has been set to 140 A with an inter-pass temperature of approximately 50 °C.

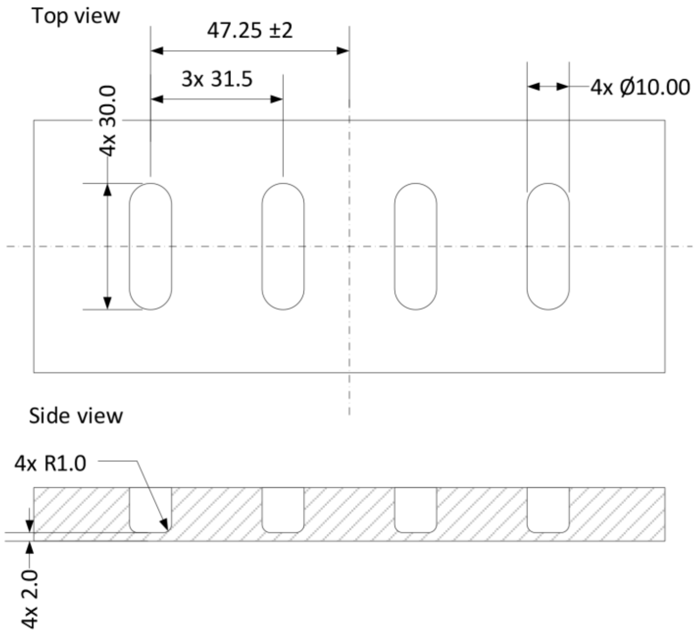

Figure 3: Dimensions and location of the weld grooves on the plates

From each weld 6 cross sections have been cut out along the filled grooves and mounted in hot mounting resin for automated metallographic preparation. All samples have been electrolytically etched with 10 wt.-% oxalic acid at 3 V DC for 3-5 seconds, followed by visual inspection using a light optical microscope at 200x magnification. The location of imperfections has been recorded and the crack length been measured along the centre line of the crack. The data is presented as total crack length (TCL) averaged over 4 grooves. Microhardness has been measured on representative samples with an applied force of 0.5 kgf (HV0.5), for which a Shimadzu HMV-2 microhardness tester has been used. Electron microscopy has been used for phase identification and high resolution image acquisition. A Leo 1550 FEG SEM has been used in conjunction with an Oxford Instruments EDS detector. Grain size has been measured on two cross sections per condition on base metal microstructure using three circles superimposed over recorded images. Unlike for general microstructural characterisation the samples were etched with 10 wt.-% nitric acid at 1.7 V vs. stainless steel electrode for 20 seconds, based on the approach described in [42]. Images were taken at 12.5x magnification such that a total area of at least 1 cm2 was covered and subsequently stitched together using Photoshop CC 2015. The amount of Nb-rich secondary phases (laves and carbides) has been quantified with image analysis using ImageJ on 5 SEM images per condition. Atomic number contrast visualised by backscattered electrons (BSE) has been used to distinguish between matrix and secondary phases. Thermodynamic calculations to identify equilibrium phases have been performed using JMatPro. All measurements are presented including their respective standard deviation as a measure for the error.

2.1.2 Thermal cycle measurement

Cast plates of ATI®718PlusTM with the dimensions of 150x60x12.7 mm have been investigated. The chemical composition given in Table 1 has been used with the material being in the as cast condition with an average hardness of 415 ± 5HV0.5 and grain size of 1300 ± 300µm. The microstructure is showing typical dendritic microstructure with Nb-rich precipitates in the interdendridic areas. While in practice such a material is usually homogenized, a previous study found that as cast microstructures are more resistant to HAZ liquation cracking [43], hence the choice of material condition for this investigation.

Four linear grooves with the dimensions 30x10x10 mm, a side radius of 5 mm and a bottom radius of 1 mm have been machined into the plate, together with holes for thermocouples drilled into the backside. The schematic drawing is shown in Figure 4. The positioning of thermocouples along the sidewall of the grooves was chosen such that the thermal history of base metal HAZ could be studied as a function of weld layer deposition. On each side of the groove one thermocouple was placed at 25, 50 and 75% relative to the height of the groove, respectively. The position of the outer 2 thermocouples was reversed on one side of the groove, as indicated in Figure 4.

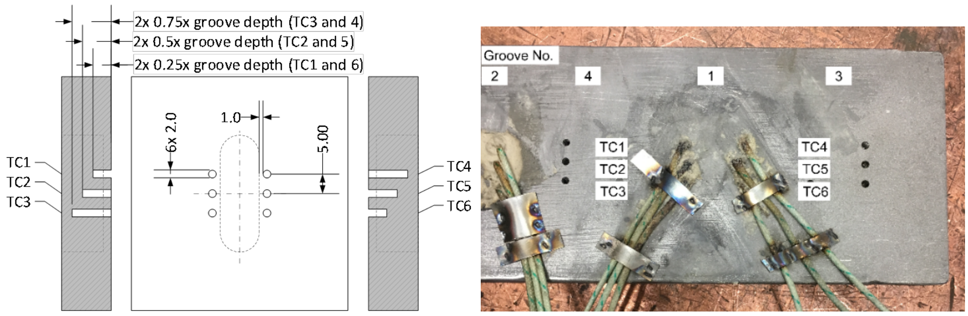

Figure 4: Dimensions and positions of holes for thermocouple placement (left), groove (backside) with attached thermocouples (right).

To achieve a stable mounting of the thermocouples within the holes, they were fixed using Omegabond® OB-400 high temperature, heat conductive cement. Movement has further been restricted by thin metal plates tack-welded onto the back of the cast plate. Type-K thermocouples with a diameter of 0.25 mm have been used in conjunction with a National Instruments NI cDAQ-9172 data logger, using a sampling rate of 10Hz.The complete setup is exemplarily shown in Figure 4, with the numbers of the grooves indicating the order they have been welded. Since the placement of thermocouples on the backside of the plate required more space than the distance between two grooves allowed, the grooves have been filled in two consecutive operations (1-2 and 3-4).

The welding has been carried out manually by an experienced welder using TIG welding with argon as shielding gas and filler wire with matching chemistry. A 20wt.-% thorium (WT-20) tungsten electrode has been used with a shielding gas flow of 15 l/min together with a 20 mm nozzle. The welding current was set to 140 A and was temporarily adjusted by the welder if required during the process (e.g. start/stop location). A large electrode stick-out has been used to be able to reach the bottom of the grooves. The welding included a root pass to create a smoother bottom radius, followed by filling the grooves lengthwise, approximately covering half the width of a groove per pass. The plate was cooled with compressed air until an inter-pass temperature of approx. 200°C was reached. The following layer was started at the previous stop location and was then following the groove wall on the opposite site (i.e. the groove was filled in a spiral motion, with interruptions every half turn).

For visual inspection after the welding 3 cross sections have been prepared for each welded groove. They were positioned such that each of them intersected two thermocouple locations (one on each side of the groove). All samples have after cutting been mounted in hot mounting resin, followed by manual grinding to reach the desired cross section location. After automatic polishing the samples then have been electrolytically etched in 10wt.-% oxalic acid at 3V DC for 3-5s and visually inspected using a stereo and light optical microscope.

2.2 HAYNES 282

Haynes® 282® has been investigated in form of a forged bar (repair welding study [44]) and rolled sheet (Gleeble study [45]). The chemical compositions are given in Table 2. Test specimens have been machined from these parts using abrasive waterjet cutting.

Table 2 Chemical composition in weight percentage of Haynes 282

	Ni	Cr	Co	Mo	Ti	Al	Fe	Mn	Si	C	B
Forged bar [44]	Bal	19.55	10.46	8.70	2.02	1.45	1.17	0.06	0.07	0.063	0.004
Rolled sheet [45]	Bal	19.49	10.36	8.55	2.16	1.52	0.37	0.05	0.05	0.072	0.005

2.2.1 Repair welding

The forged bar used in the study showed a solutionised microstructure with an ASTM 5.5 grain size (51 ± 7 µm) and a hardness of 315 ± 7 HV in the as received condition. In total, 8 discs with a thickness of 15mm were cut from the bar and subsequently heat treated in a vacuum furnace with a heating rate of 4-11°C/min and argon forced convection cooling down to 500°C to minimise precipitation (cooling rate >50°C/min). Four heat treatment conditions have been selected to investigate the influence of pre weld material condition on weld cracking during repair welding. While the heat treatment at 1010°C was chosen to just above the dissolution temperature of the γ' phase in the material (997°C [46]) without dissolving secondary carbides, the treatment at 1120°C was selected to obtain a carbide distribution similar to the one obtained by using the recommended solutionising parameters. This temperature is the lower limit of the solution annealing window, which results in the removal of M23C6 carbides (1019°C) from the grain boundaries, while M6C and MC carbides remain in the material [46, 47]. The highest temperature was used to produce a coarse grained material. The temperature represents the upper limit of the solution annealing window and together with the longer exposure time of 2h (cf. 0.5h for 1120°C) an increase in grain size could be expected. Fully age hardened material has been reported to be more susceptible to weld cracking especially when it comes to SAC due to the localisation of strain to the HAZ [28]. One disc has hence been put through a complete age hardening cycle (788°C for 8h) before being repair welded. Another four discs have been put through a post weld heat treatment after completing the repair welding operation. Direct aging has been chosen opposed to the conventionally applied heating to solution treatment temperature to subject the material to more severe conditions. The reasoning here was that direct aging results in a longer exposure time in the precipitation temperature range without heating to solution annealing temperature, where most of the stress relaxation occurs.

Five circular repair welding grooves with a diameter of 25mm, 10mm depth and a bottom radius of 5mm have been machined into the discs after the pre weld heat treatments, as indicated in Figure5a. To maximise welding restraint, the discs were fixed to 25mm thick stainless steel discs by a circumferential weld (cf. Figure5b).

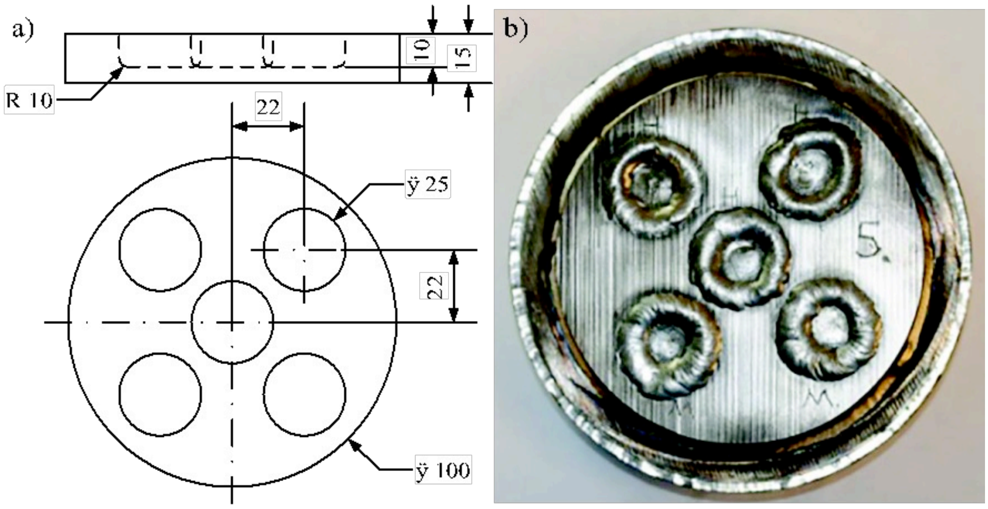

Figure 5: a Sample design. B Disc with filled grooved. Note the restraint maximising stainless steel disc welded onto the bottom of the Haynes 282 disc.

The grooves were filled with Haynes® 282® filler wire using a tungsten-2% thorium (WT-20) electrode. Ar gas has been used as shielding gas with a nozzle gas flow of 8-15l/min. A matching chemistry filler material in the form of 1.14mm wire has been used with negative polarity and two welding currents, 120 and 140A. The interpass temperature was approximately 50°C and was reached by quenching with Ar gas in between layer deposition.

2.2.2 Gleeble study

Haynes 282 in the form of rolled sheet (cf. Table 3) has been investigated using a Gleeble 3800 thermomechanical simulator. Testing parameters are shown in Table 3. Three replicates were tested at each point, resulting in a total amount of 180 tested samples.

Table 3 Gleeble test parameters

Temperature [°C]		750			800		850			900		950
Exposure time [s]	5	10	15	20	30	60	120	180	300	600	1200	1800
Heating rate [°C/s]	1000											
Cooling rate (T>500°C) [°C/s]	100											
Stroke rate [mm/s]	55											
Chamber pressure [mbar]	0.1											
Thermocouple	Type K											

Reduction in area (RA) has been used as an indicator for ductility, which has been measured using an Olympus SZX9 stereo optical microscope. The test order was randomized within repeats and specimens could only be identified via their run number to reduce the impact of boundary conditions and operational bias. Fractographic analysis has been carried out on selected specimens using a ZEISS Evo 50 scanning electron microscope (SEM), while a Leo 1550 FEG SEM has been used for high resolution image acquisition. The latter provided the basis for particle analysis via automatic image analysis with the Zeiss AxioVison Rel.4.6 software. The sample set has been limited to the 5 longest exposure times per temperature (300, 600, 1200 and 1800s) and the as received condition, with three images analysed for each specimen. The selection threshold has been manually adjusted for each picture before the particle diameter has been automatically determined by the software. JMatPro 8.0 has been used in conjunction with the nickel based superalloy database to verify the results from particle analysis.

3 Results and Analysis

3.1 ASSESSING THE WELDING BEHAVIOUR OF NEWLY DEVELOPED NICKEL BASED SUPERALLOYS

The development of Alloy 718 enabled welding as a joining technique for a wide range of applications within the aerospace sector and in related industries where high temperature stable materials have to be used for structural applications. The limited thermal stability of Alloy 718 has during the recent years led to the development of new alloys such as ATI718Plus and Haynes 282, which enable higher combustion temperatures and hence could increase the efficiency of aircraft engines and turbines used for power generation. The complex microstructure of nickel based superalloys requires profound knowledge about changes and processes going on in the material during welding. One of the latter is the formation of weld cracks, which can be hard to impossible to be avoided if no deep understanding of the underlying causes has been obtained. A recent trend in the aerospace industry is the production of large structural components out of small wrought and cast parts that are joined together by welding. Another large application of welding is the repair of such structures, as full replacement due to local imperfections is economically not feasible given the complexity of the parts. Repairs are often carried out manually, requiring highly skilled welders. The variability of manual processing further increases the complexity of the task. Studying multi pass repair welds is hence a good starting point to obtain knowledge about the material behaviour during welding, since the conditions present there are to be placed in the more severe side of the application spectrum. The repair weldability of two newly developed alloys has been investigated within this project, namely Haynes 282 and ATI178Plus.

In welding of nickel based superalloys different types of cracks can be found. These can be grouped into hot cracks such as solidification and HAZ liquation cracks and warm cracks, a category strain age cracking and ductility dip cracking fall into.

Weld solidification cracking occurs in the fusion zone, where cracks are formed during the passage of the liquid-solid two-phase region upon cooling. Several theories have been proposed during the last 60 years, but still not all aspects have been fully understood. In general, two main factors can be identified, namely the presence of restraint and a susceptible microstructure. The former can be due to the formation of thermal stresses during cooling, as a temperature and heating/ cooling rate gradient between fusion zone and base material is present. The restraint is further influenced by the weld bead geometry, workpiece design and thickness, heat input during welding and mechanical fixture (external restraint). Early theories include the shrinkage-brittleness theory [4] and the strain theory of hot tearing [5]. These have been combined to the generalised theory of super-solidus cracking by Borland in the early 1960s [6].

In contrast to weld solidification cracking, which occurs in the fusion zone of the weld, HAZ liquation cracking is localised to the partially melted zone, usually referred to as PMZ. This zone lies in the heat affected zone and is in close proximity to the fusion zone. Its main characteristic is the presence of a liquid fraction, forming when exceeding the effective solidus temperature during heating. The presence of stresses during subsequent cooling then can cause crack formation. The liquid can form by different mechanisms, namely segregation induced liquation, constitutional liquation and eutectic melting.

Segregation induced liquation is based on the local suppression of the solidus temperature. Especially elements like S, P and B are known to segregate within the microstructure and are usually enriched near grain boundaries. The segregation behaviour of these elements and their effect on the weldability has been thoroughly studied particularly for Alloy 718 [7–17]. As apart from boron, which has to be found to have a positive influence on creep and stress rupture life [48], the general effect of these elements is of detrimental nature and their concentrations are usually kept on a minimum level.

Constitutional liquation can occur if second phase particles (i.e. precipitates) are present in the matrix. The mechanism has originally been introduced for maraging steels by Pepe and Savage [18] and later been adapted to explain HAZ liquation cracking in Alloy 718 by Owczarski et al. [19]. A key factor for the mechanism is fast heating, so that particles can survive despite not being thermodynamically stable above the eutectic temperature (assuming the phase interactions can be described by a eutectic system). Under the further assumption of equilibrium conditions at the phase boundary between matrix and particle, a concentration gradient develops around the particle during its subsequent dissolution. When reaching the eutectic temperature, the reaction zone around the particle liquates. It has to be noted that the particle itself does not melt, as e.g. TiC has a melting point far above that of the nickel matrix [49] and only the solute enriched reaction zone contributes to the melt formation. This mechanism has been observed especially for Nb bearing alloys such as Alloy 718 and ALLVAC 718Plus [2, 19] but has also been reported for other precipitation hardening alloys [20–23].

Eutectic melting is only found in cast alloys and related to the strong segregation in interdendritic areas. This has been observed in cast Alloy 718 by various authors [2, 24, 25]. Related to the in general more segregated microstructure of cast alloys they have to be considered more susceptible to HAZ liquation cracking.

When it comes to repair weldability, a typical measure for general assessment is the quantification of weld cracks in the material. This can be done either by non-destructive tests such as e.g. ultrasonic inspection techniques or via investigation of weld cross sections. The latter method, while more labour intensive, has the advantage of enabling further analysis of found cracks. This can then be used to identify the cause of the crack formation and consequently this knowledge can be used to prevent failure in future welding trials.

3.1.1 Repair welding of ATI 718Plus

The analysis of weld cross sections of cast ATI 718Plus has revealed an influence of base metal microstructure on the HAZ cracking response, with post-cast solutionising heat treatments leading to an increased total crack length [40]. No clear trend was evident regarding cracks in the fusion zone, as can be seen in Figure6 a and b.

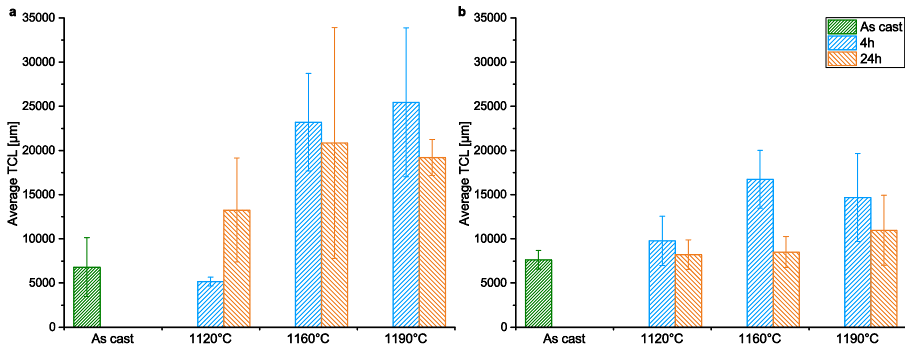

Figure 6: Total crack length (TCL) in the HAZ (a) and FZ (b) of cast ATI 718Plus with different base metal heat treatment history.

The reason behind the reduced weldability of heat treated material has been found to be related to the amount of secondary phases in the base material. While the solutioninsing treatments carried out at 1120, 1160 and 1190°C for 4 and 24h did lead to a significant reduction of Nb-rich secondary phases in the microstructure (and hence to a more homogenized material), more cracks appeared during the repair welding operation.

Upon closer inspection it became evident that with reduced secondary phase volume fraction the average crack length got increased. Figure7 shows two pictures taken in the base metal heat affected zone of material heat treated at 1120 for 4h (a) and b 1190 for 24h (b). The difference in secondary phase fraction can clearly be seen, as well as the difference in crack length.

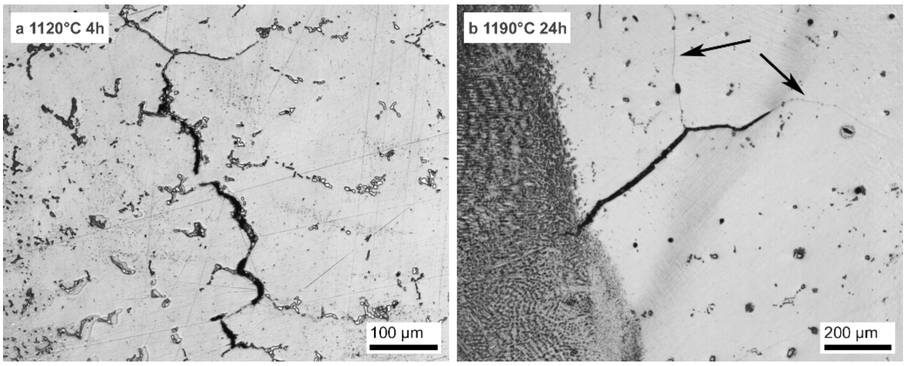

Figure 7: HAZ liquation cracks in heat treated base material, showing a transition of crack location from interdendritic areas so solidification grain boundaries present from the casting process, as indicated by arrows: a 1120°C 4h, b 1190°C 24h. Note the difference in scale and crack length.

The crack formation transitions from short, unconnected cracks in the interdendritic areas towards long cracks on solidification grain boundaries present from the casting process. The reasoning here is that the presence of low melting Nb-rich phases in interdendritic areas material in the as cast condition and, to a lesser extent, after a heat treatment at 1120°C for 4h enables the distribution of load and crack formation to a larger area and hence leads to an improved cracking response.

Cast material has to be put through a solutionising heat treatment before being put into service due to the strong segregation present in the microstructure which causes non-uniform mechanical properties. Such treatments are usually carried out in conjunction with hot isostatic pressing (HIP) to simultaneously remove porosity. The results of the repair welding study indicate that carrying out the solutionising treatment after the welding process and hence welding the material in the as cast state could reduce cracking in the HAZ. The practical applicability is however limited since cast parts are often joined with wrought parts that would require different heat treatments to prevent uncontrolled grain growth. Nevertheless, the findings do provide a better understanding of the ongoing mechanisms in cast ATI 718Plus and contribute to the knowledge needed to successfully apply this new alloy in aerospace applications.

3.1.2 Repair welding of Haynes 282

Haynes282, showed a vastly different behaviour when subjected to a multi- pass repair welding operation [44]. Irrespective of welding parameters that have been applied in the study (with 120A welding current being typical welding conditions and 140A representing a more severe environment), no cracks were present in the base metal heat affected zone. Instead, all cracking was confined to the fusion zone. No correlation between base metal heat treatment history and cracking response could be observed. Instead, the cracking response was strongly influenced by the heat input, with the use of 140A welding current leading to a 1.5x more cracks in the weld deposit layers, as visible in Figure8.

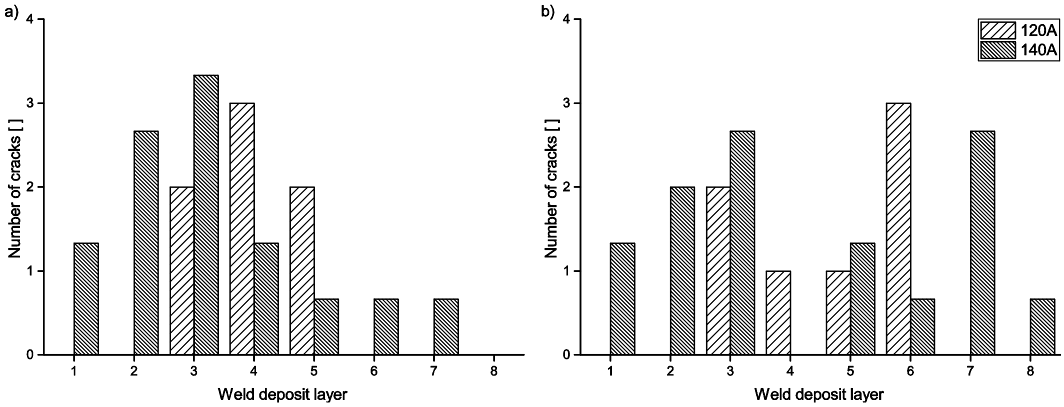

Figure 8: Total number of cracks per weld deposit layer. a Pre weld heat-treated discs (1-4). b Pre + post weld heat treated discs (5-8). Results for 140A are normalized to account for differences in sampling size for the two conditions.

It furthermore can be observed that the cracking response is independent of both pre weld microstructure and post weld heat treatments (cf. total number of cracks in Figure8 a and b). Further supported by microstructural analysis showing a dendritic structure on the crack surfaces and the location on solidification grain boundaries the cracks were classified as solidification cracks as shown in Figure 9.

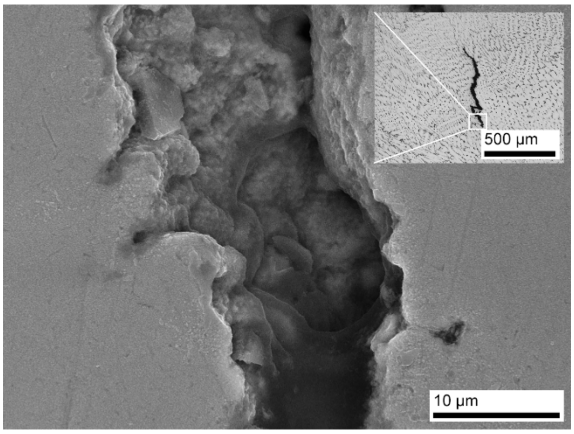

Figure 9: Solidification crack in a sample welded with 120A welding current. Clear indication of a dendritic structure in the crack opening. Crack length 706µm.

Small voids without signs of liquid phases being present were also found in the fusion zone layers. These voids were initially considered to be potential strain age cracks, EDS analysis however revealed the presence of aluminium-rich oxides. This led to the assumption that the voids are in fact oxide layers present from the welding process which have not been properly removed, cf. Figure 10

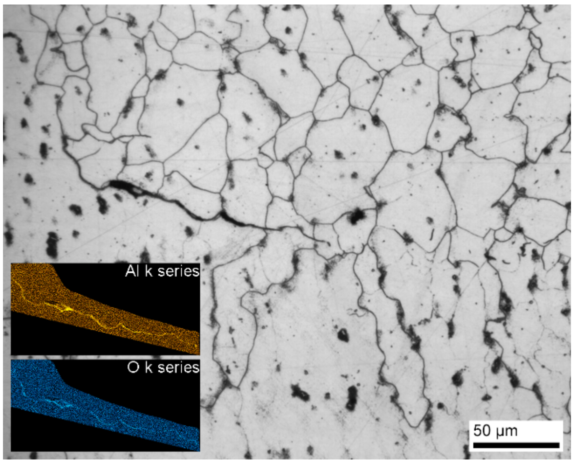

Figure 10: Aluminium-rich oxide layer ad a presumed start location (140A welding current). Void size 184µm.

Hardness measurements in both fusion zone layers and base metal HAZ revealed that 3-4 weld deposit layers are necessary for the hardness to exceed 300 HV in the weld metal. The heat affected zone showed the same trend, but a slightly quicker hardening response, with only two weld deposit layers being required. The absence of strain age cracks in the material suggests that either the weld residual stresses were below a critical level or that the hardening response was too slow for SAC to occur in the material.

The two repair welding studies indicate that SAC is not a major concern and instead liquation and solidification cracking has to be expected when welding these alloys. This is a good sign for the application of these alloys as a replacement for Alloy 718. Nevertheless, the mechanism of SAC and the resistance of candidate alloys for future application in the aerospace sector need to be further investigated. This is especially important with view on the recent trend to introduce additive manufacturing techniques into the production of engine and turbine components. With processes like selective laser melting (SLM) there is the risk of crack formation during post built processing, with strong similarities to welding related problems such as SAC.

3.2 DEVELOPMENT OF A TESTING APPROACH TO ASSESS SUSCEPTIBILITY TOWARDS STAIN AGE CRACKING

Over the years, several testing methods have been developed to assess the susceptibility towards strain age cracking and to understand underlying mechanisms. A review of the available literature was able to identify a promising testing approach, enabling material screening and the relative comparison of different alloys [38]. When it comes to weldability testing, the vast amount of testing procedures, often specifically developed during an investigation, makes the comparison of results difficult. One of the more commonly used testing approaches follows the idea of simulating the slow heating to PWHT, combined with acquiring ductility data in the temperature range where SAC occurs. This test is referred-to as constant heating rate test (CHRT) [50]. Here the samples were first pre-heated to a temperature below the aging temperature range (593°C). From there, sub- sequent heating was carried out with a constant rate of 14-17°C/min to simulate a post-weld heat treatment. The samples have then been pulled to fracture at various temperatures in the aging temperature range. The used strain rate of 0.6mm/min until yield and 2.5mm/min until fracture resulted in a short exposure time as compared to the heating procedure. This test has been used by different researchers over the years and slight modifications have been made to adapt it to modern testing equipment and its increased capabilities of physical simulation of thermal cycles [25, 37, 51, 52]. While for the original CHRT a clamshell furnace was used, the use of the Gleeble thermomechanical simulator enables fast heating and cooling cycles that are comparable to those present during welding. This results in the ability to add a fast heating and cooling cycle in advance of the CHRT part to create a microstructure similar to that found in the HAZ of welds where SAC occurs. Such a modified testing procedure has been proposed as part of the previous KME 506 project [37], with the thermal cycle schematically shown in Figure 11.

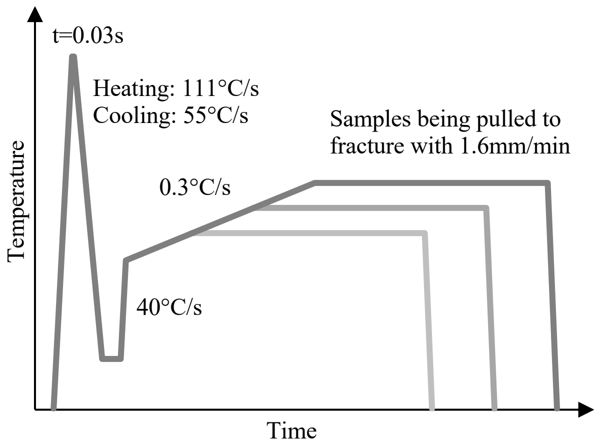

Figure 11: Schematic temperature cycle of the modified controlled heating rate test. Figure taken from [38].

The continuation of SAC research within KME 706 enabled this testing procedure to be applied to different nickel based superalloys, namely Alloy 718, ATI 718Plus and Haynes 282 [25]. Figure 12 exemplarily shows the results for Haynes282, with the characteristic drop in ductility being visible.

The modified constant heating rate test takes advantage of the more capable testing equipment that is nowadays available in welding research. The test enables the screening of different alloys based on their susceptibility towards strain age cracking. The testing of microstructures corresponding to those found in the heat affected zone of actual welds ensures that the test results can be related to results found in application. While requiring a metallographic investigation of tested samples, testing HAZ simulated microstructures furthermore includes the effect of potential weaknesses such as liquation cracks that can form during the welding process. The effect of such a pre-damaged microstructure has been found to negatively affect the material performance during simulated PWHT cycles.

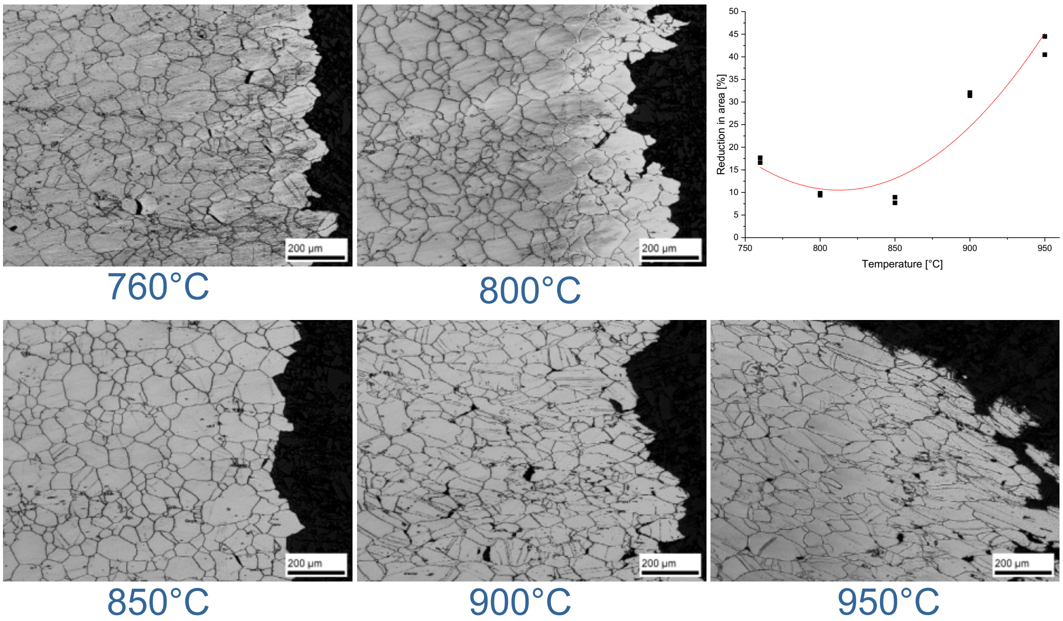

Figure 12: Deformation behaviour of Haynes 282 tested at different temperature in the modified CHRT. More brittle behaviour indicates temperature range with higher risk of cracking.

3.3 DEVELOPMENT OF A TESTING APPROACH TO CORRELATE SAC SUSCEPTIBILITY TO CHANGES IN THE MICROSTRUCTURE

With the modified CHRT being developed for screening purposes, it comes short in providing insight into mechanisms ongoing in the material. To be able to relate the material response to the CHRT to microstructural changes, a new testing procedure has been developed within the framework of KME 706 [45]. The general observation of the CHRT, the loss of ductility in the intermediate temperature range, has been taken as a starting point for the test design. With the loss in ductility being not as severe for alloys with reduced amount of hardening elements such as Al and Ti, the susceptibility to SAC strongly depends on alloy composition [25, 52, 53]. Following from that an interrelationship of ductility and precipitation kinetics has been proposed [28], but no quantified data is available yet.

Since the CHRT uses a constant heating rate to the different test temperatures, the effect of hardening reactions cannot be investigated. The new approach hence utilises fast heating of 1000°C/s and subsequent isothermal exposure (5, 10, 15, 20, 30, 60, 120, 180, 300, 600, 1200, 1800s) to obtain microstructures with varying precipitation structure. Figure 13 shows the test matrix selected to investigate Haynes 282. The test temperatures have been selected based on the results of a previous CHRT investigation such that the test covers the temperature range around the drop in ductility [25]. In the constant heating rate test (CHRT), the total exposure time in the precipitation temperature range is 20-30min, considering both the heating and mechanical testing parts of the test [52, 53]. Hence, the two longest exposure times were considered to reflect comparable conditions to those of the CHRT.

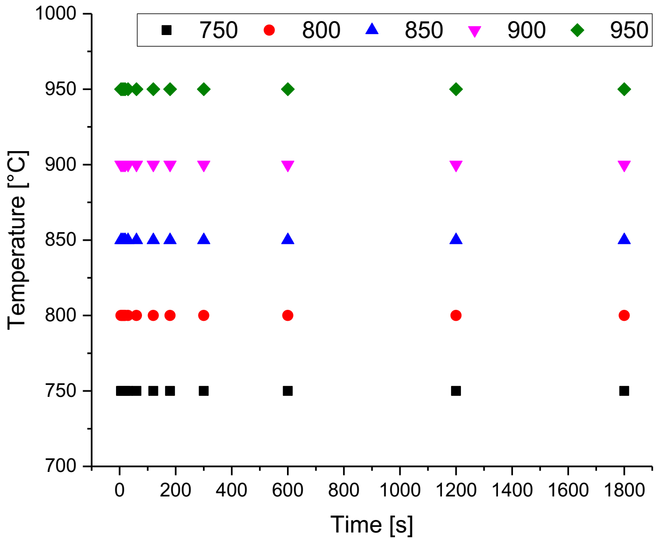

Figure 13: Test temperatures and exposure times used to investigate the effect of hardening precipitates on the ductility of Haynes282.

To be able to run the test setup in a Gleeble system, the specimen geometry used in previous investigations had to be revised. The resistance heating combined with water-cooled jaws used in this system causes a strong temperature gradient. This can lead to off-centre fracture when using test specimens with constant gauge width, since hardening reactions occurring in the centre may shift the fracture location to an area where less hardening reactions took place. This problem has previously been recognised, and two approaches were followed to solve the problem. While Norton and Lippold used steel jaws with lower heat conduction than the standard copper ones [54], Metzler used a modified specimen geometry with a constant radius to compensate for lower material strength away from the specimen centre [52]. This investigation follows the latter approach with the general concept of using a radius rather than a constant-width gauge section. Since the desired specimen geometry differed from Metzlers in size and radius, additional finite element (FE) simulations were carried out using MSC Marc. Plastic deformation has been modelled with the specimen area 4mm around the centre being heated to a temperature of 850°C while allowing free heat flow to the outer specimen side. Outside the heated section material parameters corresponding to a solutionised state have been used while in the centre section values for fully age hardened material were applied. This was assumed to represent the most severe conditions as being present after prolonged exposure time. Using different material parameters was necessary since otherwise fracture would always occur in the area with the highest temperature applied. The results shown in Figure 14 clearly indicate that the revised specimen geometry improves the likelihood that test specimens will fail at the thermocouple location in the centre during testing and hence can be used for further analysis.

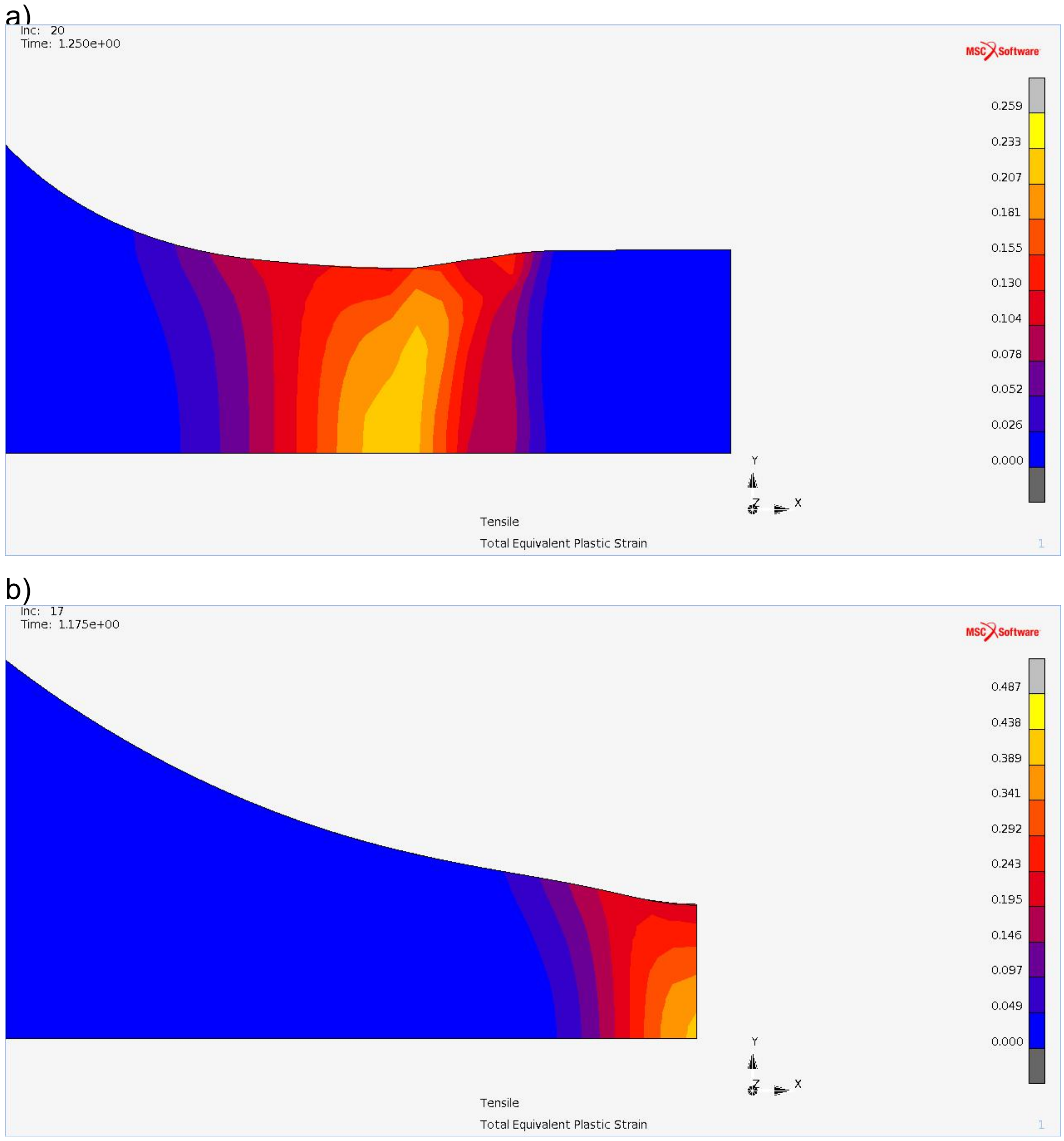

Figure 14: Simulated total equivalent plastic strain for (a) specimen with constant gauge width and (b) specimen geometry using a constant radius.

The results of the Gleeble tests show a clear influence of exposure time on the ductility, as indicated in Figure 15. This loss in ductility could be attributed to the difference in precipitation structure in the material, as hardness values correlate well with the observed ductility. Further microscopic analysis enabled the quantification of hardening phases and as such can provide viable insight into critical exposure times in the intermediate temperature range. When used as a screening test for different alloys this test furthermore has the potential to be used to develop threshold criteria for post weld heat treatment procedures in terms of heating rate and hence exposure time in the critical temperature range.

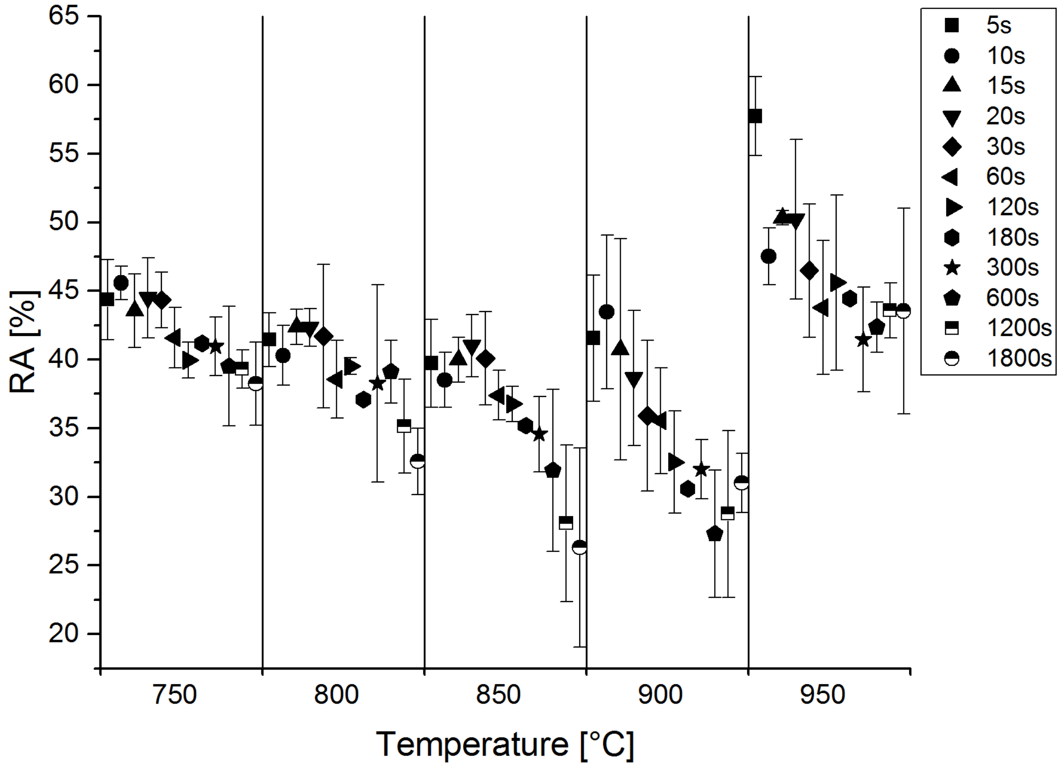

Figure 15: Reduction in area as a function of temperature and time. Average of three measurements with respective 95% confidence interval.

Results from SAXS/WAXS measurements carried out in-situ during heat treatment at 760 and 820°C furthermore provided new data on the precipitation kinetics in Haynes 282 [55], which can be used to explain the material behaviour observed in the SAC temperature range.

3.4 MEASUREMENT OF THE THERMAL CYCLE IN THE BASE METAL HAZ DURING MULTI PASS REPAIR WELDING

Using information obtained from manual repair welding studies is often not trivial due to the various parameters that cannot or only in certain limits be controlled. Weld cracking is strongly dependent on the microstructure and hence the knowledge of the thermal cycle during multi pass weld operations can provide valuable insight into ongoing mechanisms. Furthermore, such thermal data can be used for physical simulation experiments, which can complement general simulative tests as the ones discussed above. Based on the repair welding study on ATI 718Plus, a method to acquire thermal data during multi-pass manual repair welding has been developed [56].

The frequency of peak temperatures experienced from the different thermocouples during the welding of the grooves is shown in Figure 16. With knowledge of the thermal cycle during a multi pass welding operation such a test setup can be used as a starting point for controlled microstructure simulation in a Gleeble system. However, for future application the test setup has to be further developed to avoid the shortcomings observed in the current approach: The manual and hence not controlled torch movement made the correlation of data from different thermocouples difficult.

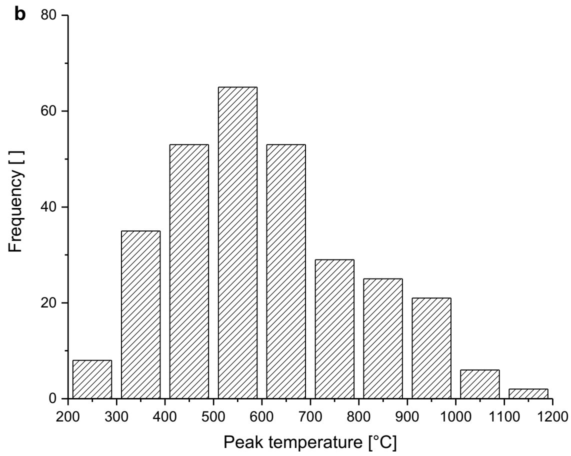

Figure 16: Distribution of peak temperature during welding, combining all thermocouples placed alongside the groove sidewalls.

Furthermore, the thermocouples could only be placed 2mm away from the side wall surface. A modified test setup with placing thermocouples along a line perpendicular to the welding groove sidewalls could mitigate the observed problems and hence provide better results for further microstructure simulation.

4 Conclusions

- The literature has been reviewed with focus on strain age cracking and related testing methods. Based on this the following conclusions can be drawn
    - With the general mechanism being accepted in literature, there is still little data available that links material response (i.e. low ductility) and quantified information about the precipitation kinetics causing it
    - Out of the numerous testing procedures that have been developed, the constant heating rate test (CHRT) seems to be most promising as a screening test. In light of more modern testing equipment some modifications could improve its results
- While both being gamma prime hardening alloys, ATI 718Plus and Haynes 282 show a very different response to multi-pass weld operations
    - Base material thermal history strongly affects the HAZ cracking response in cast ATI 718Plus, which has been found to be linked to the presence of low-melting Nb-rich phases
    - Wrought Haynes 282 shows good HAZ cracking resistance, while solidification cracking can be a concern depending on process parameters such as heat input
- Testing procedures to assess the susceptibility towards strain age cracking have been developed and applied to investigate the SAC mechanism.
    - With the modified constant heating rate test it is possible to screen materials and to compare their relative resistance towards SAC while testing is carried out on microstructures corresponding to those present in the HAZ of welds
    - The interrelationship of precipitation kinetics and the susceptibility towards SAC can be investigated with a newly developed Gleeble-based testing procedure.
    - The drop in ductility responsible for the occurrence of strain age cracking has been correlated to the hardening response and precipitate structure of Haynes 282
- Via the measurement of the thermal cycle in the HAZ during multi pass welding operations it is possible to obtain temperature data for microstructural simulations

5 Goal fulfilment

The overall goal was to obtain fundamental knowledge about weld cracking mechanisms in precipitation hardening nickel based superalloys. In view of the ongoing need for high temperature stable materials this is of great interest for the participating industrial partners. This goal was planned to be achieved via the combination of extensive metallurgical investigations and the development of reliable testing procedures.

The set goal has to be considered as fulfilled, with the objectives defined in the project plan being achieved:

- Extensive weldability studies have been carried out on newly developed alloys
- The effect of different microstructure conditions on weld cracking has been evaluated
- A measurement procedure has been designed to capture the thermal cycle during multi pass welding operations to enable the physical simulation of microstructures for better understanding of the material response to welding.
- A screening test capable of creating relative material rankings with regard to SAC resistance has been developed and successfully applied
- The effect of precipitation kinetics on microstructure and susceptibility towards strain age cracking has been investigated, for which a new testing procedure has been developed.
- The project led to the submission of 8 papers
- The project led to collaboration with different national and international partners, strengthening existing networks.

6 Suggestions for future research work

The project was able to increase the knowledge about weld cracking phenomena. The complex microstructure of superalloys and the still existing research gap when it comes to weldability data for newly developed alloys highly suggest to continue the work carried out within KME 706. It is recommended that a future project would set focus on the physical simulation of weld and HAZ microstructures to provide further insight into ongoing mechanisms via in depth microstructural analysis. This is especially interesting for the newly developed alloys such as ATI 718Plus and Haynes 282 in their cast form due to their potential application in aerospace industry and the scarce availability of weld data for these new materials.

7 Literature references

1. Sjöberg G (2010) Casting Superalloys For Structural Applications. In: 7th International Symposium on Superalloy 718 and Derivatives. The Minerals, Metals & Materials Society, pp 117–130

2. Andersson J (2011) Weldability of precipitation hardening superalloys: Influence of microstructure. Doctoral Thesis, Chalmers University of Technology

3. Sims CT, Stoloff NS, Hagel WC (1987) Superalloys II. Wiley, New York

4. Pumphrey WI, Jennings PH (1948) A Consideration of the Nature of Brittleness at Temperatures Above the Solidus in Castings and Welds in Aluminium Alloys. J Inst Met 75:235–256

5. Pellini WS (1952) Strain Theory of Hot Tearing. Foundry 80:125-133;192-199

6. Borland JC (1960) Generalized Theory of Super-Solidus Cracking in Welds (and Castings). Br Weld J 7:508–512

7. Andersson J (2005) Allvac 718+, Mikrostruktur vid Värmebehandling och Svetsning. Bachelor Thesis, Bergskolan - The Swedish School of Mining and Metallurgy

8. Kelly TJ (1989) Elemental effects on cast 718 weldability. Weld J 68:44s–51s

9. Chaturvedi MC, Chen W, Saranchuk A (1997) The Effect of B Segregation on Heat-Affected Zone Microfissuring in EB Welded Inconel 718. In: Superalloys 718, 625, 706 and Various Derivatives. The Minerals, Metals & Materials Society, pp 743–751

10. Vishwakarma KR, Chaturvedi MC (2009) Effect of boron and phosphorus on HAZ microfissuring of Allvac 718 Plus superalloy. Mater Sci Technol 25:351–360 . doi: 10.1179/174328407X243032

11. Vincent R (1985) Precipitation around welds in the nickel-base superalloy, Inconel 718. Acta Metall 33:1205–1216

12. Thompson RG, Dobbs JR, Mayo DE (1986) The Effect of Heat Treatment on Microfissuring in Alloy 718. Weld J 65:299s-304s

13. Huang X, Chaturvedi MC, Richards NL, Jackman J (1997) The effect of grain boundary segregation of boron in cast alloy 718 on HAZ microfissuring—A SIMS analysis. Acta Mater 45:3095–3107 . doi: 10.1016/S1359-6454(97)00017-7

14. Ping DH, Gu YF, Cui CY, Harada H (2007) Grain boundary segregation in a Ni–Fe-based (Alloy 718) superalloy. Mater Sci Eng A 456:99–102 . doi: 10.1016/j.msea.2007.01.090

15. Chen W, Chaturvedi MC, Richards NL (2001) Effect of boron segregation at grain boundaries on heat-affected zone cracking in wrought INCONEL 718. Metall Mater Trans A 32:931–939

16. Benhadad S, Richards NL, Chaturvedi MC (2002) The influence of minor elements on the weldability of an INCONEL 718-type superalloy. Metall Mater Trans A 33:2005–2017

17. Alam T, Felfer PJ, Chaturvedi M, et al (2012) Segregation of B, P, and C in the Ni-Based Superalloy, Inconel 718. Metall Mater Trans A 43:2183–2191 . doi: 10.1007/s11661-012-1085-9

18. Pepe JJ, Savage WF (1967) Effects of Constitutional Liquation in 18-Ni Maraging Steel Weldments. Weld J 46:411s-422s

19. Owczarski WA, Duvall DS, Sullivan CP (1966) A Model for Heat-Affected Zone Cracking in Nickel-Base Superalloys. Weld J 45:145s-155s

20. Vishwakarma K (2008) Microstructural Analysis of Weld Cracking in 718 Plus Superalloy. University of Manitoba

21. Radhakrishnan B, Thompson RG (1993) The effect of weld Heat-Affected zone (HAZ) liquation kinetics on the hot cracking susceptibility of alloy 718. Metall Trans A 24:1409–1422

22. Ojo OA, Richards NL, Chaturvedi MC (2004) Contribution of constitutional liquation of gamma prime precipitate to weld HAZ cracking of cast Inconel 738 superalloy. Scr Mater 50:641–646 . doi: 10.1016/j.scriptamat.2003.11.025

23. Ojo OA, Richards NL, Chaturvedi MC (2004) Liquid film migration of constitutionally liquated γ' in weld heat affected zone (HAZ) of Inconel 738LC superalloy. Scr Mater 51:141–146 . doi: 10.1016/j.scriptamat.2004.03.040

24. Baeslack WA, Nelson DE (1986) Morphology of weld heat-affected zone liquation in cast alloy 718. Metallography 19:371–379

25. Hanning F (2015) Strain Age Cracking of Nickel Based Superalloys. Master Thesis, Chalmers University of Technology

26. Hughes WP, Berry TF (1967) A Study of the Strain-Age Cracking Characteristics in Welded René 41 - Phase I. Weld J 46:361s-370s

27. Wu KC, Herfert RE (1967) Microstructural Studies of René 41 Simulated Weld Heat-Affected Zones. Weld J 46:32s-38s

28. Prager M, Shira CS (1968) Welding of Precipitation-Hardening Nickel-Base Alloys. WRC Bull 128:1–55

29. Duvall DS, Owczarski WA (1969) Studies of Postweld Heat-Treatment Cracking in Nickel-Base Alloys. Weld J 48:10s-22s

30. Dix AW, Savage WF (1971) Factors influencing strain-age cracking in Inconel X-750. Weld J 50:247s-252s

31. McKeown D (1971) Re-Heat Cracking in High Nickel Alloy Heat-Affected Zones. Weld J 50:201s-206s

32. Franklin JE, Savage WF (1974) Stress Relaxation and Strain-Age Cracking in Rene 41 Weldments. Weld J 53:380s-387s

33. Thamburaj R, Goldak JA, Wallace W (1979) The Influence of Chemical Composition in Post-Weld Heat Treatment Cracking in René 41. SAMPE Q 4:6–12

34. Rhines FN, Wray PJ (1961) Investigation of the Intermediate Temperature Ductility Minimum of Metals. ASM Trans Q 54:

35. Younger RN, Baker RG (1961) Heat-Afected Zone Cracking in Welded Austenitic Steels During Heat Treatment. Br Weld J 8:579–587

36. Schwenk W, Trabold AF (1963) Weldability of René 41. Weld J 42:460s-645s

37. Andersson J (2014) Weldability of Ni-Based Superalloys. In: Proceedings of the 8th International Symposium on Superalloy 718 and Derivatives. The Minerals, Metals & Materials Society, pp 249–262

38. Hanning F, Andersson J (2016) A Review of Strain Age Cracking in Nickel Based Superalloys. In: Conference Proceedings of the 7th International Swedish Production Symposium. Lund, SE

39. Thamburaj R, Wallace W, Goldak JA (1983) Post-weld heat-treatment cracking in superalloys. Int Met Rev 28:1–22 . doi: 10.1179/imtr.1983.28.1.1

40. Hanning F, Andersson J (2018) The influence of base metal microstructure on weld cracking in manually GTA repair welded cast ATI 718Plus®. In: Proceedings of the 2018 Superalloy 718 & Derivatives: Energy, Aerospace, and Industrial Applications. The Minerals, Metals & Materials Society, Pittsburgh, USA, p submitted manuscript

41. Andersson J, Sjöberg G, Hänninen H (2011) Metallurgical Response of Electron Beam Welded Allvac 718PlusTM. In: Hot Cracking Phenomena in Welds III. Springer Berlin Heidelberg, pp 415–429

42. Hanning F, Engelberg DL (2014) Metallographic screening of grain boundary engineered type 304 austenitic stainless steel. Mater Charact 94:111–115 . doi: 10.1016/j.matchar.2014.05.016

43. Andersson J, Sjöberg G, Larsson J (2010) Investigation of Homogenization and its Influence on the Repair Welding of Cast Allvac 718Plus. In: Proceedings of the 7th International Symposium on Superalloy 718 and Derivatives. The Minerals, Metals & Materials Society, pp 439–454

44. Hanning F, Andersson J (2018) Weldability of wrought Haynes® 282® repair welded using manual gas tungsten arc welding. Weld World 62:39–45 . doi: 10.1007/s40194-017-0508-z

45. Hanning F, Steffenburg-Nordenström J, Andersson J (2018) The effect of exposure time on the ductility of wrought Haynes® 282® in the temperature range of 750-950°C. Manuscript

46. Pike LM (2006) HAYNES® 282™ Alloy - A New Wrought Superalloy Designed for Improved Creep Strength and Fabricability. In: Proceedings of ASME Turbo Expo 2006: Power for Land, Sea and Air. ASME, Barcelona, Spain, pp 1031–1039

47. Haynes International Inc. (2008) Haynes 282 Product Brochure

48. Cao W-D, Kennedy RL (1997) Effect and Mechanism of Phosphorous and Boron on Creep Deformation of Alloy 718. In: Superalloys 718, 625, 706 and Various Derivatives. pp 511–520

49. DuPont JN, Lippold JC, Kiser SD (2009) Welding metallurgy and weldability of nickel-base alloys. Wiley, Hoboken, N.J.

50. Carlton JB, Prager M (1970) Variables Influencing the Strain-Age Cracking and Mechanical Properties of René 41 and Related Alloys. WRC Bull 150:13–23

51. Rowe MD (2006) Ranking the resistance of wrought superalloys to strain-age cracking. Weld J 85:27s-34s

52. Metzler DA (2008) A Gleeble®-based method for ranking the strain-age cracking susceptibility of Ni-based superalloys. Weld J 87:249s-256s

53. Fawley RW, Prager M (1970) Evaluating the Resistance of René 41 to Strain-Age Cracking. WRC Bull 150:1–12

54. Norton SJ, Lippold JC (2003) Development of a Gleeble-Based Test for Postweld Heat Treatment Cracking Susceptibility. In: 6th International Trends in Welding Research Conference Proceedings. ASM International, pp 609–614

55. Haas S, Andersson J, Fisk M, et al (2018) Correlation of precipitate evolution with Vickers hardness in Haynes® 282® superalloy: In-situ high-energy SAXS/WAXS investigation. Mater Sci Eng A 711:250–258 . doi: 10.1016/j.msea.2017.11.035

56. Hanning F, Hurtig K, Andersson J (2018) Measurement of the thermal cycle in the base metal heat affected zone of cast ATI®718PlusTM during manual multi-pass TIG welding. In: 8th Swedish Production Symposium, SPS 2018. Stockholm, Sweden

8 Publications

Andersson J (2014) Weldability of Ni-Based Superalloys. In: Proceedings of the 8th International Symposium on Superalloy 718 and Derivatives. The Minerals, Metals & Materials Society, pp 249–262

Hanning F (2015) Strain Age Cracking of Nickel Based Superalloys. Master Thesis, Chalmers University of Technology

Hanning F, Andersson J (2016) A Review of Strain Age Cracking in Nickel Based Superalloys. In: Conference Proceedings of the 7th International Swedish Production Symposium. Lund, SE

Hanning F, Andersson J (2018) Weldability of wrought Haynes® 282® repair welded using manual gas tungsten arc welding. Weld World 62:39–45 . doi: 10.1007/s40194-017-0508-z

Hanning F, Andersson J (2018) The influence of base metal microstructure on weld cracking in manually GTA repair welded cast ATI 718Plus®. In: Proceedings of the 2018 Superalloy 718 & Derivatives: Energy, Aerospace, and Industrial Applications. The Minerals, Metals & Materials Society, Pittsburgh, USA, **submitted manuscript**

Hanning F, Rashidi M, Steffenburg-Nordenström J, Andersson J (2018) The effect of exposure time on the ductility of wrought Haynes® 282® in the temperature range of 750-950°C. **in manuscript**

Hanning F, Hurtig K, Andersson J (2018) Measurement of the thermal cycle in the base metal heat affected zone of cast ATI®718PlusTM during manual multi-pass TIG welding. In: 8th Swedish Production Symposium, SPS 2018. Stockholm, Sweden, **submitted manuscript**

Andersson J (2018) Review of weldability of precipitation hardening Ni- and Fe-Ni.based superalloys. In: Proceedings of the 2018 Superalloy 718 & Derivatives: Energy, Aerospace, and Industrial Applications. The Minerals, Metals & Materials Society, Pittsburgh, USA, **submitted manuscript**

Haas S, Andersson J, Fisk M, et al (2018) Correlation of precipitate evolution with Vickers hardness in Haynes® 282® superalloy: In-situ high-energy SAXS/WAXS investigation. Materials Science and Engineering: A 711:250–258 . doi: 10.1016/j.msea.2017.11.035

Weldability of nickel-base superalloys for energy applications

The aim of the project has been to establish knowledge about weldability assessment of Ni-based superalloys. This aim has been broken down into several objectives: to assess weldability of Ni-based superalloys; Establish knowledge about factors that influence the susceptibility towards strain age cracking (SAC); Investigate general susceptibility of new alloys towards SAC; developing a testing rationale that can provide deeper understanding of ongoing mechanisms; assess how influencing factors can be controlled and how SAC can be prevented.

The results show that weld cracking behaviour is highly alloy specific and no generalized approach is possible to prevent cracking during welding of superalloys. More specifically, ATI 718Plus is more susceptible towards HAZ liquation cracking than Haynes 282, while for the latter the concern was mainly solidification cracking.

The strain age cracking susceptibility of different alloys has been investigated, with Haynes 282 showing comparable resistance to Alloy 718. Furthermore, the precipitation characteristics of Haynes 282 could be correlated to the low ductility responsible for strain age cracking to occur via a newly developed testing procedure.

Energiforsk is the Swedish Energy Research Centre – an industrially owned body dedicated to meeting the common energy challenges faced by industries, authorities and society. Our vision is to be hub of Swedish energy research and our mission is to make the world of energy smarter. www.energiforsk.se

Energiforsk